JOURNAL OF GUIDANCE, CONTROL, AND DYNAMICS
Vol. 18, No. 6, November–December 1995

Robust Closed-Loop Control Design for Spacecraft Slew Maneuver Using Thrusters

Brij N. Agrawal* and Hyochoong Bang†
U.S. Naval Postgraduate School, Monterey, California 93943

In this paper, a closed-loop switching function for on–off thruster firings is proposed to provide good attitude control performance in the presence of modeling errors for single-axis slew maneuver of a rigid spacecraft and to eliminate double-sided thruster firings. The size of a single-sided deadband in the switching function provides the capability of a tradeoff between maneuver time and fuel expenditure. The application of this switching function for the single-axis slew maneuvers of flexible spacecraft is also analyzed. The analytical simulations and experimental results demonstrate that the proposed switching function provides significant improvement in the slew maneuver performance.

Nomenclature

I^*	= estimated parameter of moment of inertia I
I^*/N^*	= $\gamma I/N$
N^*	= estimated parameter of thruster torque N
γ	= estimation error factor
$\gamma_{\min}$	= $1-0.01\sigma$
$\gamma_{\max}$	= $1+0.01\sigma$
σ	= magnitude of percentage uncertainty in parameter

I. Introduction

SLEW maneuvers of flexible spacecraft have received significant attention during the past decade.[1–4] The performance criteria are minimization of fuel expenditure, slew time, and vibration of flexible structures. Different control schemes have been proposed for the corresponding control objectives.[1–8] These control laws, however, have been primarily open-loop approaches and have been used for single-axis slew maneuvers.

Singh et al.[5] solved a minimum-time slew problem analytically for the planar maneuvers of a flexible structure. The open-loop switching times are functions of the system parameters and are antisymmetric with respect to half-maneuver time for a rest-to-rest slew maneuver. Vander Velde[6] and Hablani[7] developed maneuver strategies for zero residual energy. In all these formulations, however, modeling errors are not considered, which is a major drawback of most open-loop control actions. Liu and Wie[8] have proposed an open-loop switching law to enhance the robustness of the control in the presence of modeling errors. The increased number of switchings turned out to contribute to minimizing errors due to modeling uncertainties. The major drawback of the open-loop control schemes, as discussed earlier, is that they are sensitive to modeling errors and unmodeled external disturbances. Also, the practical implementation of these control laws usually involves considerable amount of difficulty. Therefore, there is a need to develop simple and easy-to-apply closed-loop control schemes for slew maneuvers of spacecraft using on–off thrusters. For a rigid spacecraft with zero modeling errors, the switching function for a minimum-time slew maneuver is well known. The input torque for a rest-to-rest maneuver profile is antisymmetric with acceleration during the first half and deceleration during the second half of the maneuver.

In this paper, a new closed-loop switching function for single-axis slew maneuver of a rigid body is developed. The proposed switching function accommodates generic modeling errors and unknown external disturbances. Furthermore, the paper includes experimental and analytical results for slew maneuver of the flexible spacecraft simulator (FSS) located at the Naval Postgraduate School using a classical and the modified switching function.

Received Feb. 23, 1994; revision received Dec. 13, 1994; accepted for publication Jan. 27, 1995.

*Professor, Department of Aeronautics/Astronautics. Associate Fellow AIAA.

†Research Assistant Professor, Department of Aeronautics/Astronautics. Member AIAA.

II. Rigid-Body Case

System Without Modeling Errors

For a rigid body undergoing a single-axis slew maneuver, the equation of motion is given by

$$I\ddot{\theta} = u \tag{1}$$

where I is the moment of inertia with respect of the rotational axis, θ is a rotational angle, and $-N \le u \le N$ is the applied external torque. With the boundary conditions

$$\theta = \theta_0, \qquad \dot{\theta} = 0 \qquad \text{at} \qquad t = 0$$

$$\theta = \theta_f, \qquad \dot{\theta} = 0 \qquad \text{at} \qquad t = t_f \qquad \theta_f > \theta_0$$

the minimum-time (t_f) solution for a rest-to-rest maneuver is the bang-bang law, which is antisymmetric about the half-maneuver time,[9] as

$$u = \begin{cases} N & \text{if} \quad 0 \le t \le t_f/2 \\ -N & \text{if} \quad t_f/2 < t \le t_f \\ 0 & \text{if} \quad t_f < t \end{cases} \tag{2}$$

In addition, the maneuver time t_f is given by

$$t_f = \sqrt{4I(\theta_f - \theta_0)/N} \tag{3}$$

The control law of Eq. (2) can be written in the feedback form as

$$u(t) = -N \operatorname{sgn}[s(t)] \tag{4}$$

where $s(t)$ is the switching function and has the form

$$s(t) = \tilde{\theta} + \frac{I\dot{\theta}|\dot{\theta}|}{2N}, \qquad \tilde{\theta} = \theta - \theta_f$$

and sgn is the signum function. The switching function $s(t)$ for $0 < t \le (1/2)t_f$ is given by

$$s(t) = \frac{N}{I}t^2 - \theta_f + \theta_0, \qquad \dot{s}(t) = \frac{2N}{I}t = 2\dot{\theta} \tag{5}$$

and for $(1/2)t_f < t \le t_f$,

$$s(t) = 0_+, \qquad \dot{s}(t) = 0 \tag{6}$$

Figure 1 shows the plot of $\theta, \dot{\theta}, u$, and $s(t)$ as functions of time during the slew maneuver. The slew maneuver consists of two parts.

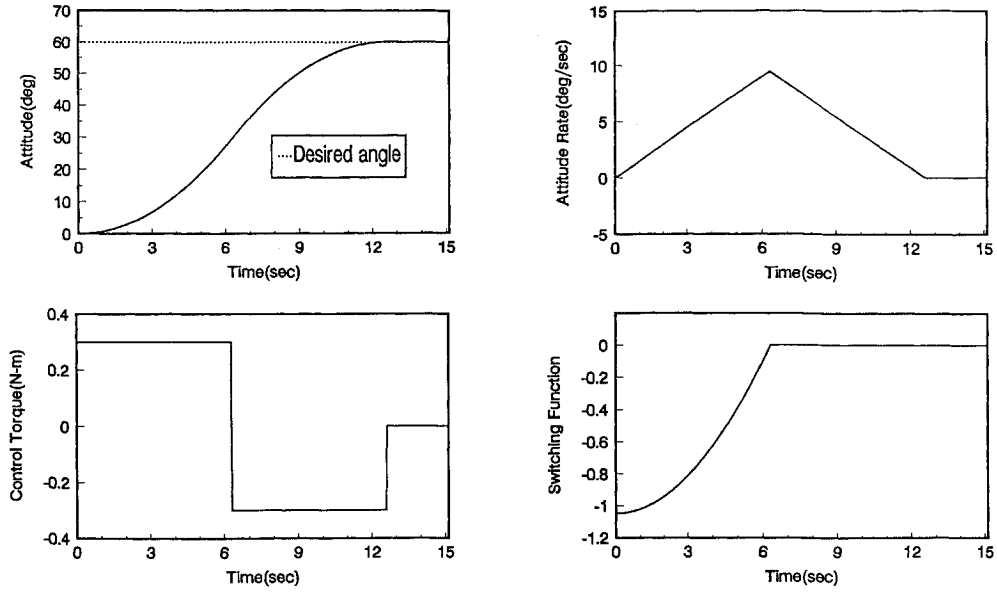

Fig. 1 Ideal minimum-time slew maneuver of rigid body.

In the first half, the body is accelerated. In the second half, it is decelerated to satisfy the prescribed boundary conditions. In the ideal case without modeling errors, the minimum-time rigid-body maneuver can be implemented by using either the open-loop torque profile or the closed-loop switching function. As is the case, the closed-loop approach is preferred over the open-loop one in practical applications. The switching function $s(t)$ is associated with two parameters, i.e., mass moment of inertia I and thruster level N.

System with Modeling Errors

Now let us analyze the robustness of the switching function. Let us consider that there is an error in the estimation of inertia I and/or the thruster level N. It should be noted that disturbance torque can be considered as an error in the estimation of the thruster level N. The switching function can be rewritten as

$$\begin{aligned} s_\gamma(t) &= \tilde{\theta} + \frac{I(1+\epsilon_1)}{2N(1+\epsilon_2)}\dot{\theta}|\dot{\theta}| \\ &= \tilde{\theta} + \frac{I^*}{2N^*}\dot{\theta}|\dot{\theta}| \\ &= \tilde{\theta} + \gamma\frac{I}{2N}\dot{\theta}|\dot{\theta}| \end{aligned} \tag{7}$$

where $\gamma \equiv (1+\epsilon_1)/(1+\epsilon_2)$ represents the modeling error factor and I^* and N^* are estimated values of I and N, respectively, being equal to $I(1+\epsilon_1)$ and $N(1+\epsilon_2)$. The new switching function $s_\gamma(t)$ has the following characteristics. let t_1 be the time when the switching function $s_\gamma(t)$ reaches zero. It is given by

$$t_1 = \sqrt{2I(\theta_f - \theta_0)/N(1+\gamma)} \tag{8}$$

For $0 \le t \le t_1$ and $u(t) = N$,

$$s_\gamma(t) = \frac{N}{2I}t^2(1+\gamma) - \theta_f + \theta_0 \tag{9}$$

$$\dot{s}_\gamma(t) = \frac{Nt}{I}(1+\gamma) \tag{10}$$

From Eq. (10), $\dot{s}_\gamma$ will be positive for all values of γ greater than -1. Therefore, s_γ will continue to increase, from a negative value, until it reaches a zero value. The time t_1 will be greater than $1/2t_f$ for $\gamma < 1$ and less than $1/2t_f$ for $\gamma > 1$.

For the second half of the slew maneuver, s_γ remains 0_+, a positive small perturbation from zero value, for $\gamma = 1$, representing absence of modeling errors. We want to analyze the impact of $\gamma \neq 1$ on $s_\gamma(t)$ during this period. We assume that $\dot{\theta} > 0$ for this period even if the same conclusions can be made for $\dot{\theta} < 0$. Differentiating Eq. (7) and using Eq. (1), we get

$$\dot{s}_\gamma = \dot{\theta} + \gamma\frac{I\ddot{\theta}}{N}\dot{\theta} = \dot{\theta}\left(1 + \gamma\frac{u}{N}\right) \tag{11}$$

In order to determine whether s_γ tracks $s_\gamma = 0$ trajectory, we calculate

$$\frac{1}{2}\frac{\mathrm{d}}{\mathrm{d}t}s_\gamma^2 = s_\gamma\dot{s}_\gamma \tag{12}$$

If the above function is negative, then s_γ tracks the $s_\gamma = 0$ trajectory; otherwise it will drift from it. For $s_\gamma < 0$, $u = N$,

$$\frac{1}{2}\frac{\mathrm{d}}{\mathrm{d}t}s_\gamma^2 = s_\gamma\dot{\theta}(1+\gamma) < 0, \qquad \text{for} \qquad \gamma > -1 \tag{13}$$

Therefore, the magnitude of $s_\gamma(t)$ decreases asymptotically, and s_γ will move toward the $s_\gamma = 0$ trajectory. For $s_\gamma > 0$, $u = -N$,

$$\frac{1}{2}\frac{\mathrm{d}}{\mathrm{d}t}s_\gamma^2 = \begin{cases} s_\gamma\dot{\theta}(1-\gamma) < 0, & \text{for} \quad \gamma > 1 \\ s_\gamma\dot{\theta}(1-\gamma) > 0, & \text{for} \quad \gamma < 1 \end{cases} \tag{14}$$

Based on Eqs. (13) and (14), it can be concluded that, for $\gamma < 1$, s_γ will drift from $s_\gamma = 0$. For $\gamma > 1$, s_γ will converge toward the $s_\gamma = 0$ trajectory.

Figure 2 shows the plot of θ, u, and s_γ for $\gamma = 0.9$ and $\gamma = 1.1$. The results show that, for $\gamma < 1$, s_γ will drift from the $s_\gamma = 0$ trajectory, resulting in overshoot of the angular position. The thruster firings are one sided during most of the maneuver time. For $\gamma > 1$, s_γ tracks the $s_\gamma = 0$ trajectory, resulting in highly accurate pointing. However, there are double-sided thruster firings that result in the increase of fuel expenditure.

In order to eliminate double-sided thruster firings, one solution is to introduce a deadband in the switching function as follows:

$$u = 0 \qquad \text{for} \qquad -\epsilon \le s_\gamma \le \epsilon \tag{15}$$

During the deadband, from Eq. (11),

$$\dot{s}_\gamma = \dot{\theta} > 0$$

For $\gamma > 1$, the following conditions apply:

$$\begin{aligned} \dot{s}_\gamma &< 0 \qquad \text{for} \qquad s_\gamma > \epsilon \\ \dot{s}_\gamma &> 0 \qquad \text{for} \qquad s_\gamma < \epsilon \end{aligned} \tag{16}$$

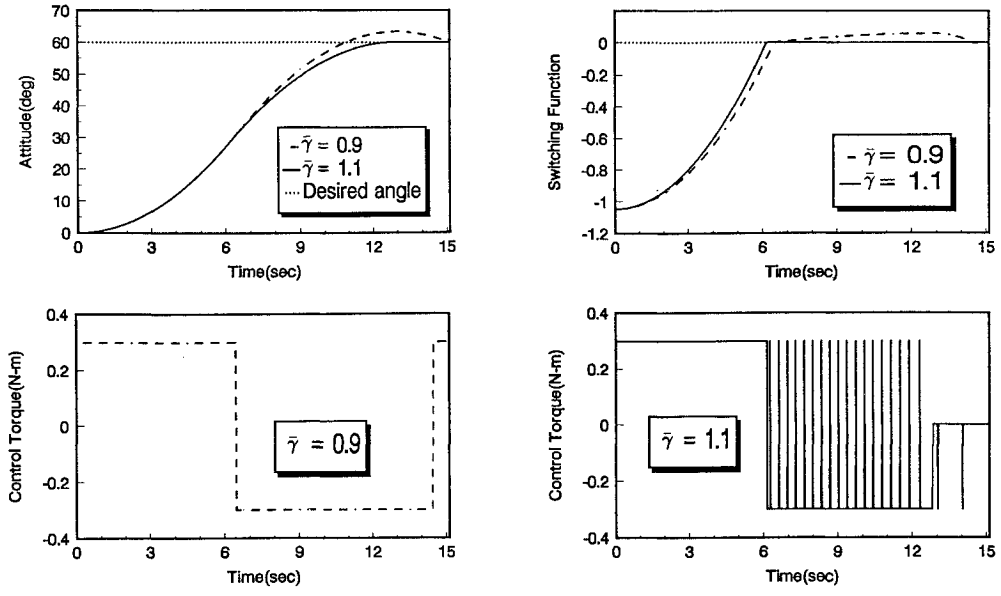

Fig. 2 Simulation results with different γs.

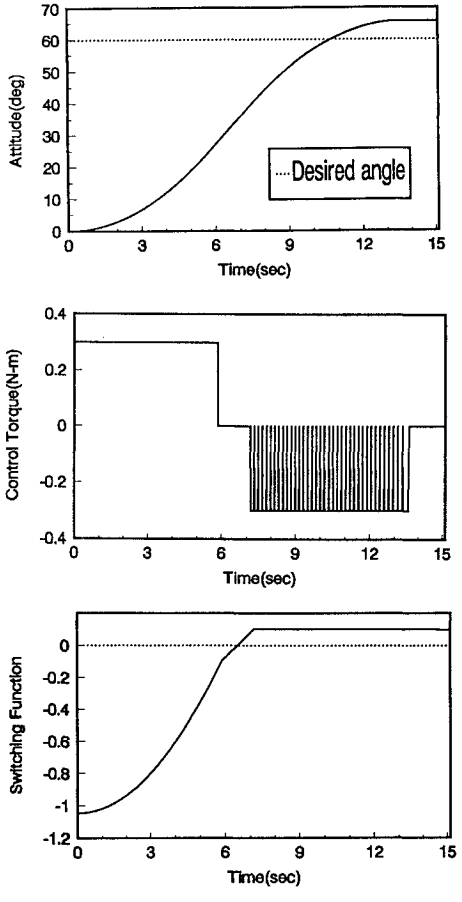

Fig. 3 Slew maneuver with double-sided deadband.

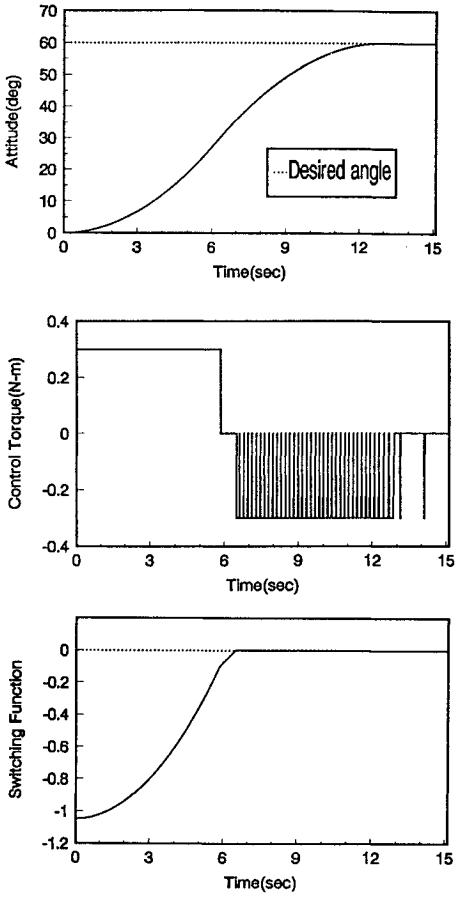

Fig. 4 Slew maneuver with single-sided deadband.

or

$$\frac{1}{2}\frac{\mathrm{d}}{\mathrm{d}t}(s_\gamma - \epsilon)^2 < 0$$

Therefore, for $\gamma > 1$, s_γ will track the $s_\gamma = \epsilon$ trajectory. This will result in single-sided firings but degraded maneuver pointing performance due to overshoot in the desired attitude and longer slew time. The larger the deadband, the poorer the pointing performance.

Figure 3 shows simulation results θ, u, and s for $\gamma = 1.1$ and $\epsilon = 0.1$. We can see that thruster firings are only single sided, but s_γ tracks the $s_\gamma = \epsilon$ trajectory and maneuver pointing performance is degraded due to overshoot in the desired attitude angle and longer slew time. To improve the maneuver pointing performance, we propose one-sided deadband in the switching function as follows:

$$u = 0 \qquad \text{for} \qquad -\epsilon \le s_\gamma < 0 \tag{17}$$

For $\gamma > 1$, the following condition applies:

$$\frac{1}{2}\frac{\mathrm{d}}{\mathrm{d}t}s_\gamma^2 < 0$$

Therefore, for $\gamma > 1$ in the one-sided deadband switching function, s_γ will track the $s_\gamma = 0$ trajectory, resulting in improved pointing performance. Figure 4 shows simulation results θ, u, and s_γ for

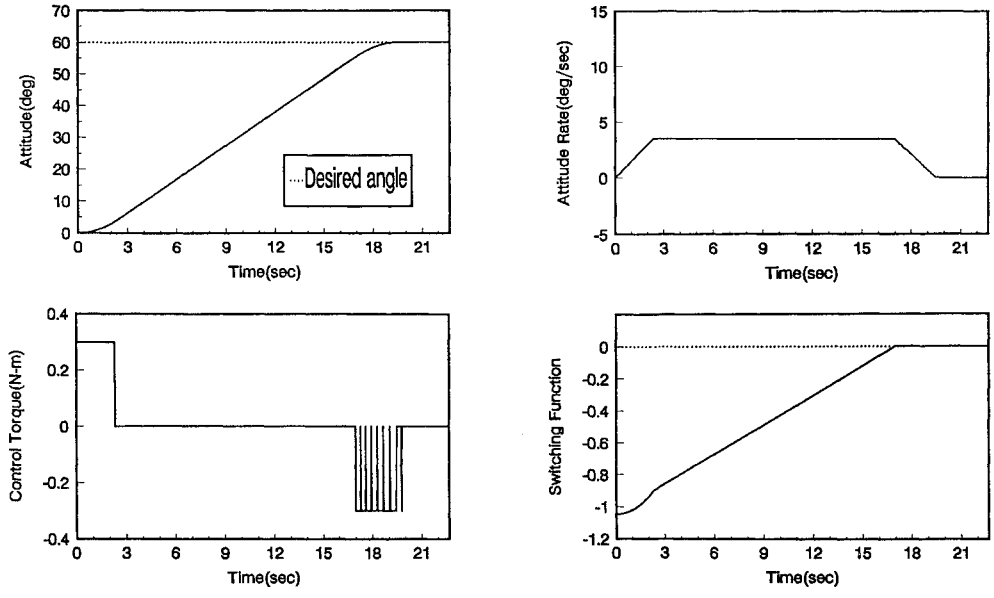

Fig. 5 Slew maneuver with large-size deadband.

$\gamma = 1.1$ and $\epsilon = 0.1$ using single-sided deadband. In this case, s_{γ} tracks the $s_{\gamma} = 0$ trajectory and shows improved maneuver pointing performance compared to the double-sided deadband.

Figure 5 shows the simulation results for a large-size deadband, $\epsilon = 0.9$. Comparing the results in Figs. 4 and 5, it can be noted that the larger deadband does not result in degradation of maneuver pointing performance, but results in an increase of slew maneuver time and a reduction in thruster firing time. Therefore, the deadband parameter in the switching function provides the capability of a tradeoff between slew maneuver time and fuel expenditure.

In summary, the above analysis shows that, in the presence of modeling errors ($\gamma \neq 1$), the classical switching function results in pointing performance degradation for $\gamma < 1$ and double-sided thruster firings for $\gamma > 1$. By introducing a double-sided deadband in the switching function, double-sided thruster firings are eliminated for $\gamma > 1$, but the pointing performance is degraded. By introduction a single-sided deadband in the switching function, we eliminate the double-sided thruster firings without degradation in the pointing performance. The size of the deadband can be selected based on a tradeoff between the slew maneuver time and propellant expenditure.

In a spacecraft design, due to spacecraft specifications, we generally know the magnitude of maximum parameter uncertainty or modeling error. Therefore, γ is given by

$$1 - 0.01\sigma \leq \gamma \leq 1 + 0.01\sigma \tag{18}$$

where σ is the magnitude of percentage uncertainty in the parameter I/N. Therefore, γ could be greater or less than unity.

Our objective is to develop a switching function for $1 - 0.01\sigma \leq \gamma \leq 1 + 0.01\sigma$ such that the performance is similar to what we achieved using the classical switching function with one-sided deadband for $\gamma > 1$, i.e., elimination of double-sided thruster firings and good pointing performance.

Proposed Switching Function

The proposed switching function is as follows for the slew maneuver of a rigid spacecraft about a single axis:

$$u = \begin{cases} -N \operatorname{sgn}[s_{\bar{\gamma}}(t)] & \text{for} \quad 0 < s_{\bar{\gamma}} \quad \text{or} \quad s_{\bar{\gamma}} < -\epsilon \\ 0 & -\epsilon \leq s_{\bar{\gamma}} \leq 0 \end{cases} \tag{19}$$

$$s_{\bar{\gamma}} = [(\theta - \theta_f) + \bar{\gamma}(I^*/2N^*)\dot{\theta}|\dot{\theta}|]$$

$$\bar{\gamma} \geq 1/\gamma_{\min}$$

By introducing $\bar{\gamma}$ such that $\bar{\gamma} \geq 1/\gamma_{\min}$ and a single-sided deadband in the switching function, we have achieved desired performance for general cases of $\gamma_{\min} \leq \gamma \leq \gamma_{\max}$, i.e., elimination of the double-sided thruster firings and good pointing performance. As mentioned earlier, external disturbance torques can be considered as errors in the thruster torque parameter N. Therefore, the switching function will provide desired performance in the presence of external disturbance torques.

The size of deadband should be selected based on a tradeoff between slew maneuver time and propellant expenditure. For a minimum-time maneuver, ϵ should be sufficiently small. For low propellant expenditure with increased maneuver time, ϵ should be large. The differences between the performance of the classical switching function and the proposed switching functions are as follows. The classical switching function provides minimum-time maneuvers in the absence of modeling errors. With the modeling errors introduced, however, the classical switching function will result in maneuver pointing performance degradation in terms of overshoot of desired attitude angle and longer slew time and/or double-sided firings in the second half of a slew maneuver.

The proposed switching function will provide good pointing performance in the presence of modeling errors and the thruster firing will be one sided during the second half of a slew maneuver. In addition, not only does the proposed switching function provide a minimum-time slew maneuver, but also, by selecting the size of the deadband, a desired tradeoff between slew time and thruster firing time can be achieved. The classical switching function is a special case of the proposed switching function with $\bar{\gamma} = 1$ and the deadband equal to zero.

There has been some related work to the proposed switching function in this paper. Zwartbol et al.[10] introduced a parameter similar to $\bar{\gamma}$ in the switching function to compensate for the disturbance torque. The selection criteria of the parameter, its influence on the performance, and relationship with modeling errors are not, however, discussed. Burdick et al.[11] used a double-sided deadband in the switching function. The single-sided deadband used in the proposed switching function is not mentioned. As discussed earlier, double-sided deadband degrades pointing performance. For a large size of deadband, to reduce fuel consumption for the maneuver, the double-sided deadband will result in unacceptable pointing performance.

III. Application to Flexible Space Structure

Next, we study the application of the proposed switching function to slew maneuvers of a flexible spacecraft model. The experimental setup (FSS) used for this study is presented in Fig. 6. It simulates the pitch axis motion of a spacecraft with a center rigid body and a reflector supported by two astro mast structures.[12,13] The simulator

consists of a central rigid body representing the spacecraft main body and a flexible appendage representing a reflector with a flexible support structure. The simulator is supported by airpads on a granite table. The center body is allowed to rotate about the vertical axis and is prevented from translational motion by an air bearing. The primary actuators are a reaction wheel and a thruster system on the central body. For this study, however, only the thruster system is used. The angular position of the central body is determined by a rotary variable differential transformer (RVDT) and the angular rate by an angular rate sensor. The thruster system is shown in Fig. 7. It consists of a 13.3-ft^3, 3000-psi supply tank connected to a pressure reducing regulator with outlet pressure range 4–250 psi. There are two thrusters providing torques in both directions. The system uses 200 psi dry air and the thruster produces 0.3 N-m torque.

The schematic representation of the model is shown in Fig. 8. It consists of a rigid body that is constrained to rotate about a fixed axis and a flexible appendage. The axes $\hat{n}_1, \hat{n}_2, \hat{n}_3$ are inertially fixed and the $\hat{n}_3$ axis represents the rotational axis. The axes $\hat{b}_1, \hat{b}_2, \hat{b}_3$ are fixed to the body and are obtained from $\hat{n}_1, \hat{n}_2, \hat{n}_3$ by a rotational angle θ about the $\hat{n}_3$ axis. The elastic deformations of a point on the flexible arms are represented by a vector $\boldsymbol{w} = [w_1, w_2]^T$ and can be written in terms of cantilever modal coordinates as

$$w_1(x,t) = \sum_{i=1}^{n} \phi_i^1(x) q_i(t)$$
$$w_2(x,t) = \sum_{i=1}^{n} \phi_i^2(x) q_i(t) \tag{20}$$

where, for the ith mode, $q_i(t)$ is the modal coordinate, ϕ_i^1 is the component of the modal vector along the $\hat{b}_1$ axis, and ϕ_i^2 is the component along the $\hat{b}_2$ axis.

The discretized finite-dimensional equations of motion for the system are given by

$$I^*\ddot{\theta} + \sum_{i=1}^{n} D_i \ddot{q}_i = u$$
$$\ddot{q}_i + \omega_i^2 q_i + D_i \ddot{\theta} = 0 \qquad i = 1, 2, \ldots, n \tag{21}$$

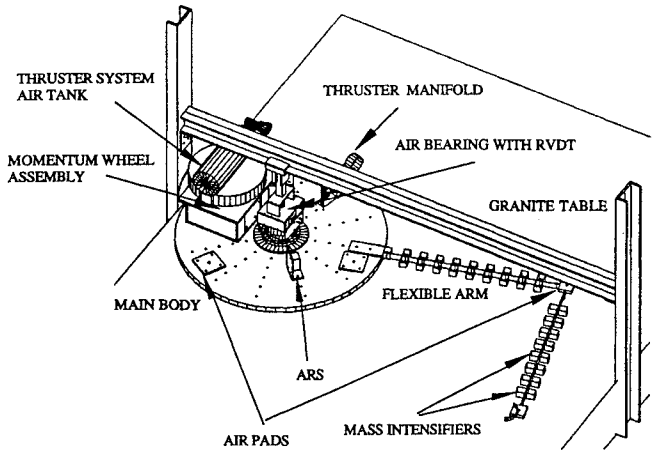

Fig. 6 Flexible spacecraft simulator.

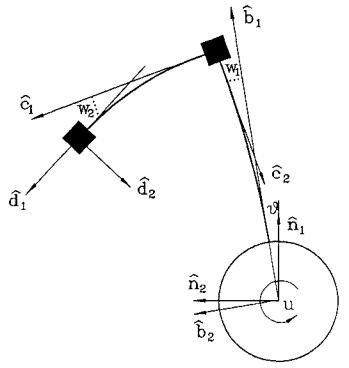

Fig. 8 Deformation and sign convention.

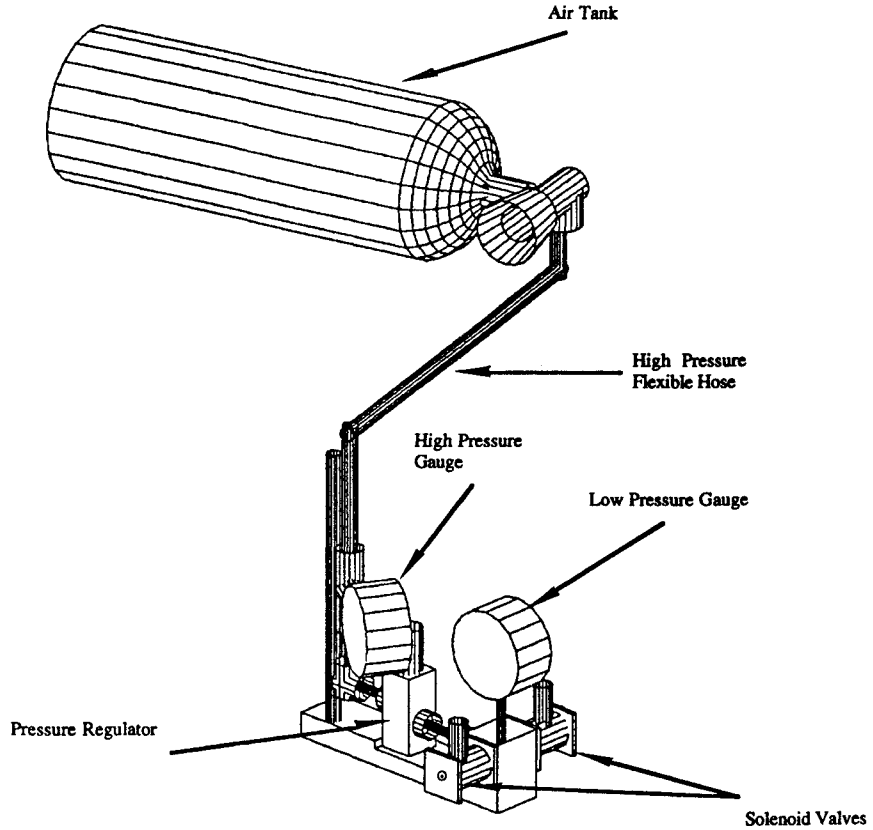

Fig. 7 Thruster system configuration.

where I^* is the estimated moment of inertia of the system about the $\hat{b}_3$ axis at the static equilibrium, ω_i is the natural frequency of the ith mode, u is the applied external torque on the body, including control and disturbance torques, and D_i is a rigid–elastic coupling term for the ith mode and is given by

$$D_i = \int_F \left(x_1 \phi_i^1 - x_2 \phi_i^2\right) \mathrm{d}m \tag{22}$$

where x_1 and x_2 are coordinate points along the $\hat{b}_1$ and $\hat{b}_2$ axes, respectively. A finite element analysis was done to determine structural cantilever frequencies and mode shapes. Table 1 gives natural frequencies for the first six flexible modes included in the analysis. The modal damping for all modes is assumed to be 0.4%.

Now we analyze the application of the proposed control law in Eq. (19) for the slew maneuver of a flexible spacecraft. By differentiating the expression for $s_{\bar{\gamma}}$ from Eq. (19) and assuming $\dot{\theta} > 0$, we get

$$\dot{s}_{\bar{\gamma}} = \dot{\theta}\left(1 + \bar{\gamma}\frac{I^*}{N^*}\ddot{\theta}\right) \tag{23}$$

From Eq. (21), we can write the expression for $\ddot{\theta}$ as

$$\ddot{\theta} = \frac{1}{I^*}\left(u - \sum_{i=1}^{n} D_i \ddot{q}_i\right) \tag{24}$$

Table 1 Natural frequencies

Mode no.	Frequency, Hz
1	0.139
2	0.420
3	2.463
4	4.295
5	6.860
6	12.820

Substituting $\ddot{\theta}$ from Eq. (24) into Eq. (23), we get

$$\dot{s}_{\bar{\gamma}} = \dot{\theta}\left[1 + \frac{\bar{\gamma}}{N^*}\left(u - \sum_{i=1}^{n} D_i \ddot{q}_i\right)\right] \tag{25}$$

Comparing the expression for $\dot{s}_{\bar{\gamma}}$ from Eq. (25) for a flexible spacecraft to that from Eq. (11) for a rigid body, we see that the expression for a flexible spacecraft has additional periodic terms due to the flexible modes. Therefore, for a flexible spacecraft, $\dot{s}_{\bar{\gamma}}$ will be oscillatory. To avoid double-sided thruster firings, during the second half of the slew maneuver, we need a larger size deadband for a flexible spacecraft. The switching curve ($s_{\bar{\gamma}} = 0$) for the rigid body is subject to dynamic couplings from the flexible motion of the arm.

IV. Simulation and Experimental Results

By using the analytical model, simulations were performed for rest-to-rest slew maneuvers of 50 deg by using the modified switching control function defined by Eq. (19). A disturbance effect of 6% of control torque magnitude was included in the simulation to create a similar environment to the actual experimental setup. Also, in order to prevent unnecessary multiple firings, a deadband around the end of the maneuver was used both in the simulation and the experiment. Simulations were performed for different values of $\bar{\gamma}$ to study their effect on attitude control performance. Figure 9 shows the plot of slew angle and thruster firings for analytical simulations with $\bar{\gamma} = 0.8, 1.0, 1.4$ without deadband. Figure 10 presents the experimental results for the slew angle and thruster firings for $\bar{\gamma} = 0.8, 1.0, 1.4$ without deadband. As expected, for higher values of $\bar{\gamma} = 1.4$, the number of double-sided thruster firings during the maneuver increases but the overshoot of the slew angle and slew time are significantly reduced. For lower value of $\bar{\gamma} = 0.8$, the number of firings decreases, but the slew angle overshoot and slew time increase. During the second half of the maneuver, the thruster

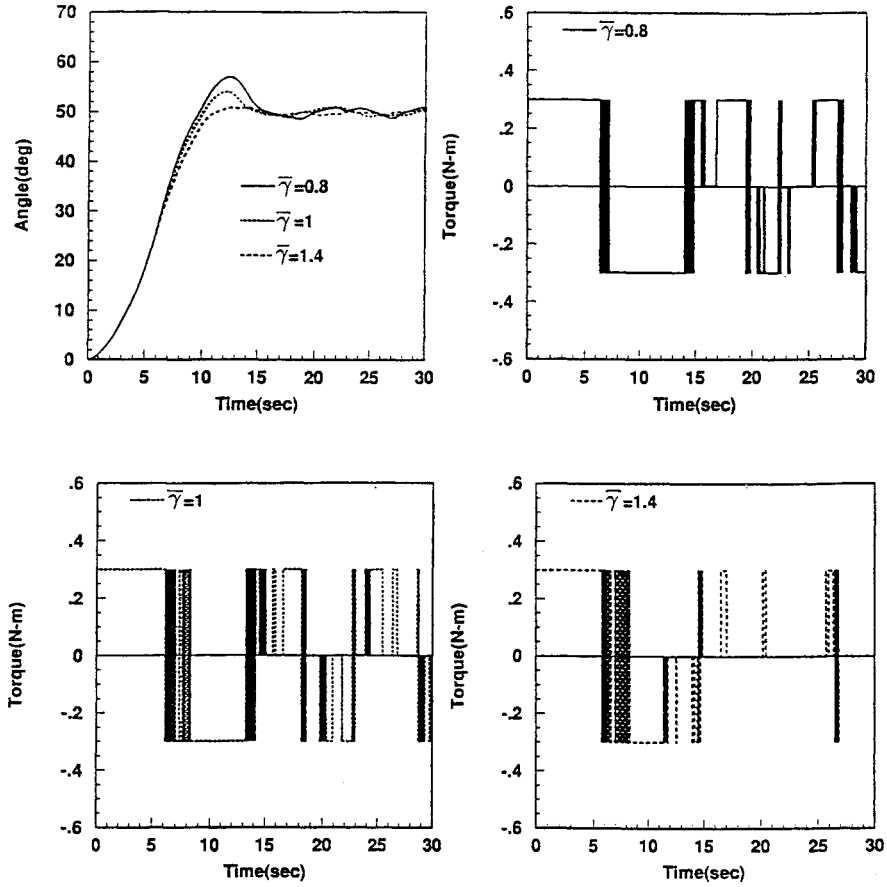

Fig. 9 Simulation results with zero deadband.

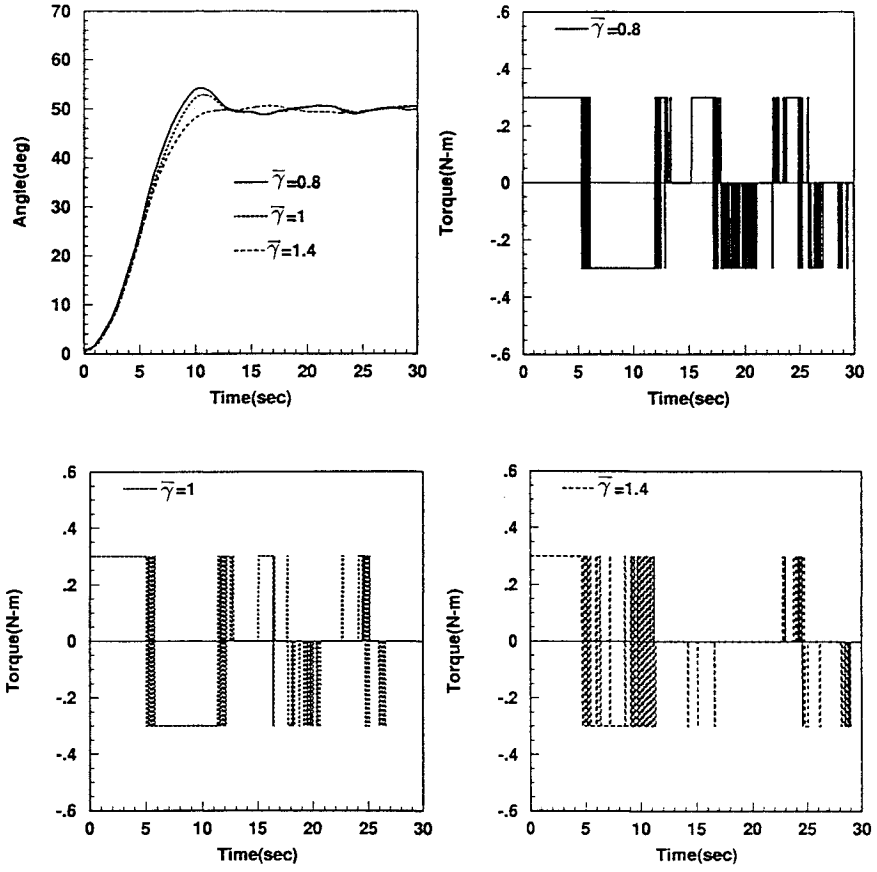

Fig. 10 Experimental results with zero deadband.

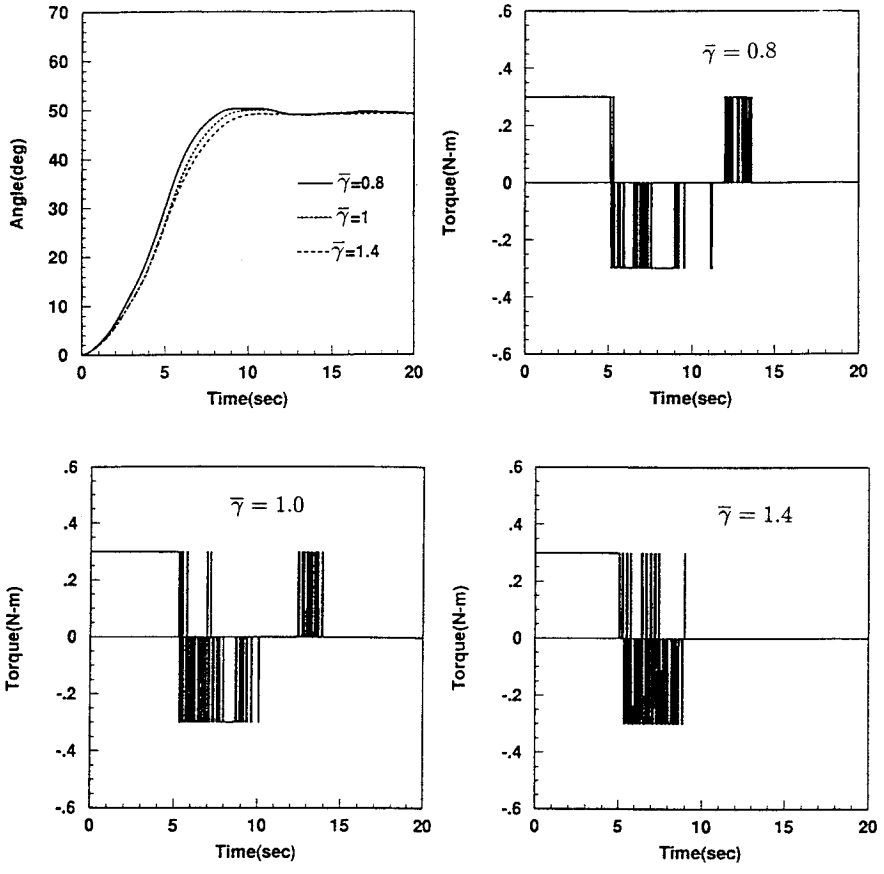

Fig. 11 Experimental results with one-sided deadband of -1.

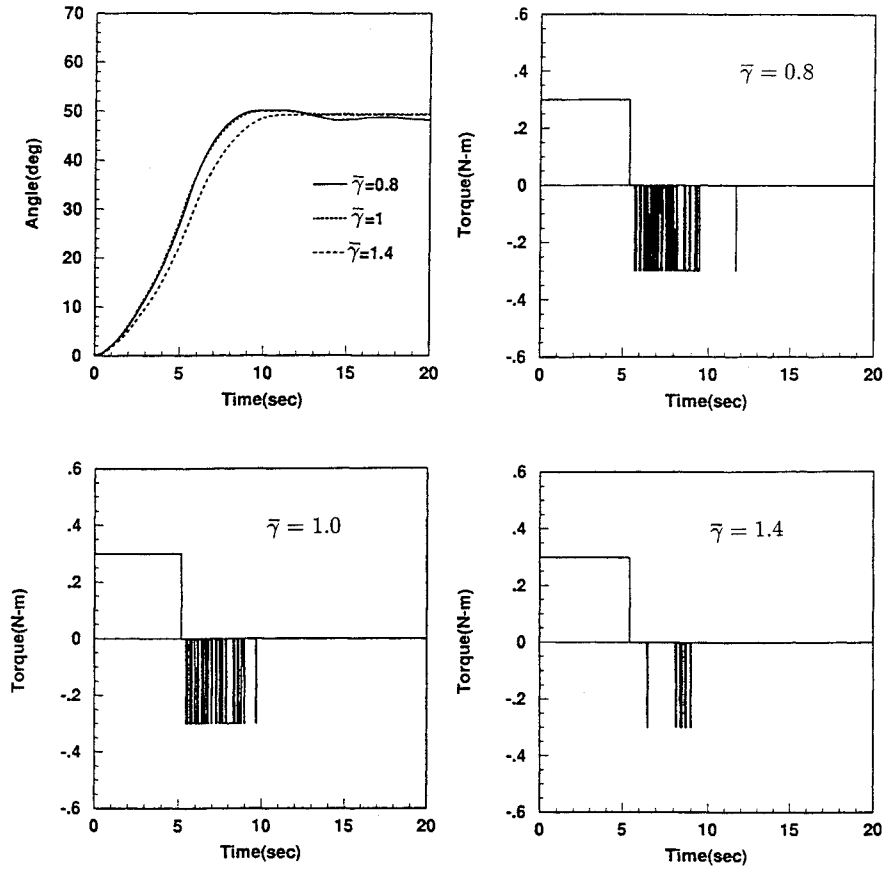

Fig. 12 Experimental results with one-sided deadband of −2.

firings are double sided for $\bar{\gamma} = 1.4$ and mainly single sided for $\bar{\gamma} = 0.8$.

Therefore, the parameter $\bar{\gamma}$ plays a significant role in the slew maneuver performance. Figure 11 shows experimental results for slew angle and thruster firings for a single-sided deadband ϵ equal to −1.0 deg and $\bar{\gamma} = 0.8, 1.0, 1.4$. The results show that, even with this deadband, thruster firings are double sided for $\bar{\gamma} = 1.0, 1.4$ during the second half of maneuver. This double-sided thruster firing will be absent for a pure rigid body and is introduced due to the flexible modes. Figure 12 shows similar experimental results for a single-sided deadband ϵ equal to −2.0 deg. In this case, the thruster firings are one sided or double-sided firings are absent for $\bar{\gamma} = 1.0, 1.4$. These results validate the earlier conclusion based on Eq. (25) that, for a flexible spacecraft, a large-size deadband in the switching function is needed to achieve single-sided thruster firings during the second half of the slew maneuver. It should be noted that the simulation results do not include minimum thruster impulse constraint.

V. Conclusions

The proposed switching function for single-axis spacecraft slew maneuver has several advantages over the classical switching function. The classical switching function does not provide robust control and is limited to minimum-time maneuvers. The presence of modeling errors will result in degradation of performance in terms of overshoot in the final desired attitude angle and longer slew time and/or double-sided thruster firings during the second half of the maneuvers. The proposed switching function provides robust control performance in the presence of modeling errors, and double-sided firings are eliminated. The single-sided deadband in the switching function is a unique feature. The double-sided deadband eliminates double-sided thruster firings but results in degradation of pointing performance. This pointing performance will be unacceptable for a large size of deadband. The single-sided deadband preserves pointing performance and eliminates double-sided thruster firings. The selection of the size of the deadband provides capability to achieve a desired tradeoff between slew maneuver time and fuel expenditure. Therefore, the proposed switching function provides robust control, high-accuracy pointing performance, elimination of double-sided thruster firings, and the flexibility of a tradeoff between slew maneuver time and fuel expenditure.

The analytical simulation and experimental results demonstrate that the proposed switching function provides good slew maneuver performance. For flexible spacecraft, however, a large-size deadband is needed in the switching function to eliminate double-sided thruster firings.

Acknowledgments

The authors express their deepest gratitude to R. Bailey, who was responsible for building the hardware involved. Also, the leading achievement by J. A. Hailey made a significant contribution to this study.

References

[1]Turner, J. D., and Junkins, J. L., *Optimal Spacecraft Rotational Maneuvers*, Elsevier Scientific, New York, 1985.

[2]Wie, B., Weiss, H., and Arapostathis, A., "Quaternion Feedback Regulator for Spacecraft Eigenaxis Rotations," *Journal of Guidance, Control, and Dynamics*, Vol. 12, No. 3, 1989, pp. 375–380.

[3]Byers, R. M., and Vadali, S. R., "Quasi Closed Form Solution to the Time-Optimal Rigid Spacecraft Reorientation Problem," *Journal of Guidance, Control, and Dynamics*, Vol. 16, No. 3, 1993, pp. 453–461.

[4]Meier, E. B., and Bryson, A. E., "Efficient Algorithm for Time Optimal Control of a Two-Link Manipulator," *Journal of Guidance, Control, and Dynamics*, Vol. 13, No. 5, 1990, pp. 859–866.

[5]Singh, G., Kabamba, P. T., and McClamroch, N. H., "Planar Time-Optimal, Rest-to-Rest Slewing Maneuvers of Flexible Spacecraft," *Journal of Guidance, Control, and Dynamics*, Vol. 12, No. 1, 1989, pp. 71–81.

[6]Vander Velde, W. E., and He, J., "Design of Space Structure Control Systems Using On-Off Thrusters," *Journal of Guidance, Control, and Dynamics*, Vol. 6, No. 1, 1983, pp. 53–60.

[7]Hablani, H. B., "Zero-Residual-Energy, Single-Axis Slew of Flexible Spacecraft Using Thrusters: Dynamics Approach," *Journal of Guidance, Control, and Dynamics*, Vol. 15, No. 1, 1992, pp. 104–113.

[8]Liu, Q., and Wie, B., "Robust Time-Optimal Control of Uncertain Flexible Spacecraft," *Journal of Guidance, Control, and Dynamics*, Vol. 15, No. 3, 1992, pp. 597–604.

[9]Athans, M., and Falb, P. L., *Optimal Control*, McGraw–Hill, New York, 1966.

[10]Zwartbol, T., Hameetman, G. J., Slippens, C. P. R. C., and Terpstra, A. P., "Experiments in Modern Control On-Board IRAS," *Proceedings of the AIAA Guidance, Navigation, and Control Conference*, AIAA, New York, 1984, pp. 302–315 (A84-43435).

[11]Burdick, G. M., Lin, H. S., and Wong, E. C., "A Scheme for Target Tracking and Pointing During Small Celestial Body Encounters," *Journal of Guidance, Control, and Dynamics*, Vol. 7, No. 4, 1984, pp. 450–457.

[12]Hailey, J. A., "Experimental Verification of Attitude Control Techniques for Flexible Spacecraft Slew Maneuvers," M.S. Thesis, U.S. Naval Postgraduate School, Monterey, CA, March 1992.

[13]Junkins, J. L., and Bang, H., "Maneuver and Vibration Control of Hybrid Coordinate Systems Using Lyapunov Stability Theory," *Journal of Guidance, Control, and Dynamics*, Vol. 16, No. 4, 1993, pp. 668–676.